IX

DESIGN OPTIMIZATION OF 3D STEEL FRAME STRUCTURES

9.1 Objectives

Two objectives are associated with this chapter. First is to ascertain the advantages, mentioned in Chapter 8, of the developed algorithm considering more complex problems. Second is to investigate the effect of the approaches, employed for determining the effective buckling length of a column, on the optimum design. This chapter therefore extends the work to the discrete optimum design of 3–dimensional (3D) steel frame structures using the modified genetic algorithm (GA) linked to design rules to BS 5950 and BS 6399. In the formulation of the optimization problem, the objective function is the total weight of the structural members. The cross–sectional properties of the structural members, which form the design variables, are chosen from three separate catalogues (universal beams and columns covered by BS 4, and circular hollow sections from BS 4848).

Chapter 2 and 3 indicate that the theory and methods for the evaluation of the effective length of columns are based on a second order analysis assuming that the buckling of members out of plane of the framework is prevented. This, however, could be correct for 3D structures as well if a rigid bracing system or shear wall, etc., is provided. Therefore, due to the need for the use of a more accurately evaluated effective buckling length of columns in 3D steel frame structures, the finite element method is employed.

Following the design procedure of steel structures to BS 5950, the minimum weight designs of two 3D steel frame structures subjected to multiple loading cases are obtained. These examples show that the modified GA in combination with the structural design rules provides an efficient tool for practicing designers of steel frame structures.

This chapter starts with describing the design procedure for 3D steel frame structures according to BS 5950, then combines that procedure with the modified GA to perform design optimization of benchmark examples.

9.2 Design procedure to BS 5950

The local and global coordinate systems shown in Figure 9.1 are assumed in order to correlate between the indices given by BS 5950 and that employed in the context. Figure 9.2a shows an isometric view of a 3D structure with coordinate system while Figures 9.2b and 9,2c display the structural system as well as the deformed configuration.

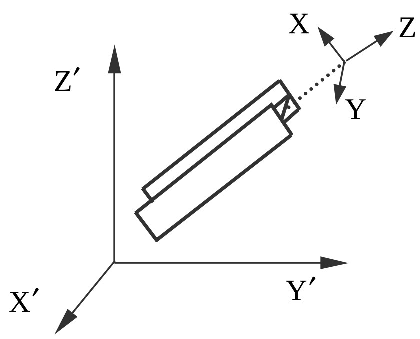

Figure 9.1. Local and global coordinate systems

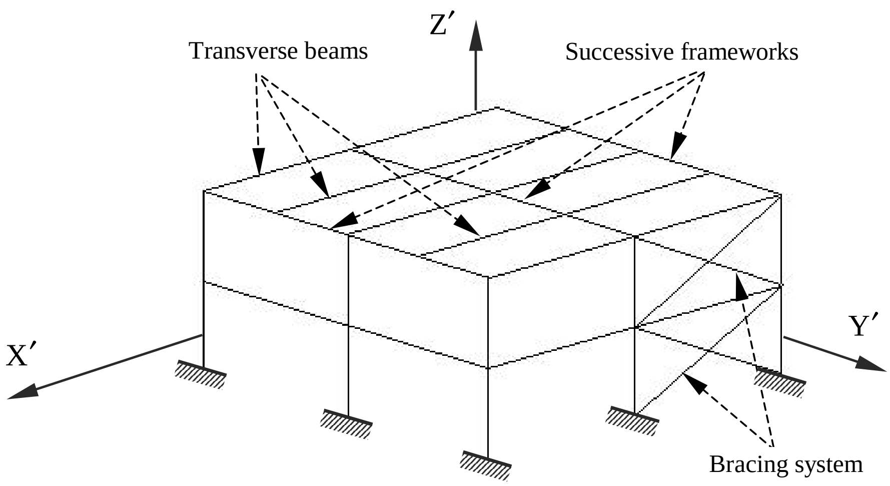

(a) Isometric view

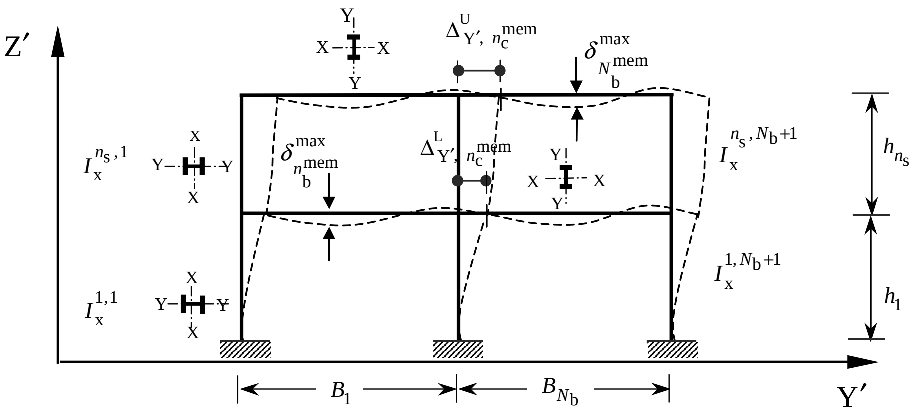

(b) Z′ – Y′ projection of the 3D structure

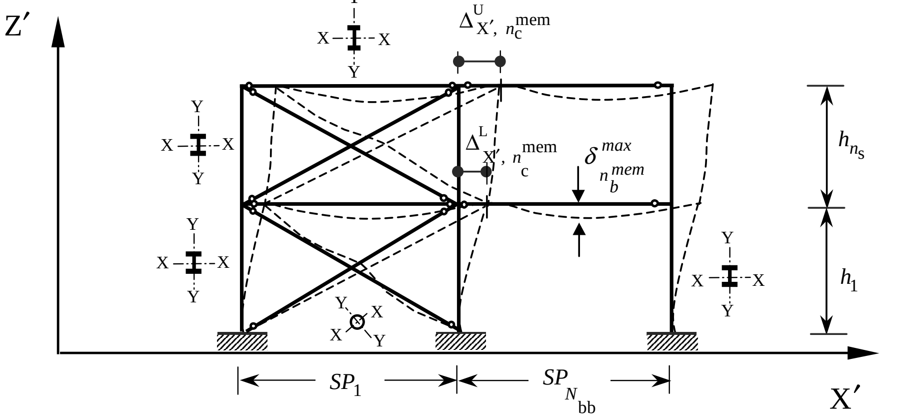

(c) Z′ – X′ projection of the 3D structure

Figure 9.2. 3D structure with the coordinate system and deformed configuration

It is assumed that the successive frameworks are rigid–jointed. In addition, it is supposed that one end of each transverse beam is free to rotate about its local axes X, Y and Z while the second end is free to rotate about X and Y axes. This assumption has been made because BS 5950 does not cater for the design of members subjected to torsional moment. Similarly, the structural system of the bracing members is considered as shown in Figure 9.2c.

BS 5950 requires the designer to select appropriate standard sections for the members of a steel structure in order to obtain a design having a sufficient factor of safety. This is accomplished by considering ultimate and serviceability limit states.

In elastic design of rigid jointed multi–storey structures, BS 5950 recommends that a linear analysis of the whole structure is carried out. This is achieved by utilising the finite element package ANSYS. Then, the design criteria are checked. This can be summarised in the following steps.

Step 1. Preparation of data files including structural geometry, loading cases, etc.

Step 2. Classification of the structure whether it is sway or non–sway. This is achieved by applying the notional horizontal loading case. A structure, analysed without including the effect of cladding, is classified as non–sway if each column of the structure satisfies

$$\frac{\left|\Delta^{\mathrm{U}}_{\mathrm{X}', n_{\mathrm{c}}^{\mathrm{mem}}}(\boldsymbol{x}) - \Delta^{\mathrm{L}}_{\mathrm{X}', n_{\mathrm{c}}^{\mathrm{mem}}}(\boldsymbol{x})\right|}{\left(\frac{L_{n_{\mathrm{c}}^{\mathrm{mem}}}}{2000}\right)} \leq 1, \tag{9.1}$$

$$\frac{\left|\Delta^{\mathrm{U}}_{\mathrm{Y}', n_{\mathrm{c}}^{\mathrm{mem}}}(\boldsymbol{x}) - \Delta^{\mathrm{L}}_{\mathrm{Y}', n_{\mathrm{c}}^{\mathrm{mem}}}(\boldsymbol{x})\right|}{\left(\frac{L_{n_c^{mem}}}{2000}\right)} \leq 1 \text{ and } n_{\mathrm{c}}^{\mathrm{mem}} = 1, \ldots, N_{\mathrm{c}}^{\mathrm{mem}}. \tag{9.2}$$

Step 3. Evaluation of the effective lengths $L^{\text{eff}}_{\text{X},\, n^{\text{mem}}}$ and $L^{\text{eff}}_{\text{Y},\, n^{\text{mem}}}$ of columns, beams and bracing members about the major (X) and minor (Y) local axes. In this work, the effective buckling length $L^{\text{eff}}_{\text{X},\, n^{\text{mem}}_{\text{c}}}$ of columns has been evaluated by the following three approaches:

- using the charts from BS 5950;
- a more accurate method (SCI, 1988) based on finite element analysis (ANSYS);
- selection of the conservative (higher) value out of the two.

In the second approach, the effective length

$$L^{\text{eff, FE}}_{\text{X},\, n^{\text{mem}}_{\text{c}}}(\boldsymbol{x}) = \frac{L_{n^{\text{mem}}_{\text{c}}}}{\sqrt{\dfrac{F_{n^{\text{mem}}_{\text{c}}}(\boldsymbol{x})}{P_{E,\, n^{\text{mem}}_{\text{c}}}}}} \tag{9.3}$$

where $F_{n^{\text{mem}}_{\text{c}}}(\boldsymbol{x})$ is the normal force at the critical load of the structure,

$$P_{E,\, n^{\text{mem}}_{\text{c}}} = \frac{\pi^2 EI_{n^{\text{mem}}_{\text{c}}}}{L^2_{n^{\text{mem}}_{\text{c}}}}\,. \tag{9.4}$$

For a beam the effective buckling length $L^{\text{eff}}_{\text{X},\, n^{\text{mem}}_{\text{b}}}$ about the X axis equals the unrestrained length of the compression flange on the underside of the beam (MacGinley, 1997).

For columns and beams, the effective length $L^{\text{eff}}_{\text{Y},\, n^{\text{mem}}}$ about the Y axis equals the unrestrained length of the member under consideration.

For bracing members, BS 5950 specifies the effective lengths $L^{\text{eff}}_{\text{X},\, n^{\text{mem}}_{\text{br}}}$ and $L^{\text{eff}}_{\text{Y},\, n^{\text{mem}}_{\text{br}}}$ depending on the end restraints of the members. In this work, it is assumed that each bracing member is not restrained at either ends about the local X axis. Therefore, $L^{\text{eff}}_{\text{X},\, n^{\text{mem}}_{\text{br}}}$ and $L^{\text{eff}}_{\text{Y},\, n^{\text{mem}}_{\text{br}}}$ can be determined by

$$L^{\text{eff}}_{\text{X},\, n^{\text{mem}}_{\text{br}}} = 1.0 L_{n^{\text{mem}}_{\text{br}}} \,, \tag{9.5}$$

$$L^{\text{eff}}_{\text{Y},\, n^{\text{mem}}_{\text{br}}} = 0.85 L_{n^{\text{mem}}_{\text{br}}} \,. \tag{9.6}$$

<u>Step 4</u>. Calculation of the slenderness ratios $\lambda_{\text{X},\, n^{\text{mem}}}(\boldsymbol{x})$ and $\lambda_{\text{Y},\, n^{\text{mem}}}(x_{i,\, j})$ of the member n^{mem} using

$$\lambda_{\text{X},\, n^{\text{mem}}}(\boldsymbol{x}) = \frac{L^{\text{eff}}_{\text{X},\, n^{\text{mem}}}(\boldsymbol{x})}{r_{\text{X},\, n^{\text{mem}}}} \,, \tag{9.7}$$

$$\lambda_{\text{Y},\, n^{\text{mem}}}(x_{i,\, j}) = \frac{L^{\text{eff}}_{\text{Y},\, n^{\text{mem}}}(x_{i,\, j})}{r_{\text{Y},\, n^{\text{mem}}}} \tag{9.8}$$

where $r_{\text{X},\, n^{\text{mem}}}$ and $r_{\text{Y},\, n^{\text{mem}}}$ are the radius of gyrations of the section member about its X and Y axes respectively.

<u>Step 5</u>. Check of the slenderness constraints $G^{\text{Sle}}_{s,\, n^{\text{mem}}}$ for each member

$$G^{\text{Sle}}_{s,\, n^{\text{mem}}}(\boldsymbol{x}) \le 1 \,,\; s = 1,\, 2, \tag{9.9}$$

where

$$G^{\text{Sle}}_{1,\, n^{\text{mem}}}(\boldsymbol{x}) = \frac{\lambda_{\text{X},\, n^{\text{mem}}}(\boldsymbol{x})}{180} \quad \text{and} \tag{9.10}$$

$$G^{\text{Sle}}_{2,\, n^{\text{mem}}}(x_{i,\, j}) = \frac{\lambda_{\text{Y},\, n^{\text{mem}}}(x_{i,\, j})}{180} \,. \tag{9.11}$$

<u>Step 6</u>. Analysis of the structure under each loading case q to obtain the normal force, shearing forces and bending moments for each member.

<u>Step 7.</u> Check of the strength criteria for each member n^{mem} under the loading case *q* as follows:

a) Determination of the type of the section of the member (e.g. slender, semi–compact, compact or plastic).

b) Evaluation of the design strength $p_{\text{y},n^{\text{mem}}}$ of the member.

c) Check of the strength constraints $G_{r,n^{\text{mem}}}^{\text{Str},q}(\boldsymbol{x})$ depending on whether the member is in tension or compression. This stage contains five checks (*r* = 5) for each member under each loading case *q*. The strength constraints are local capacity, overall capacity, shear capacities in X and Y directions and the shear buckling capacity. These can be expressed as follows:

$$G_{r,n^{\text{mem}}}^{\text{Str},q}(\boldsymbol{x}) \le 1,\ r = 1, 2, 3, 4, 5 \text{ and } q = 1,2,\Lambda\ ,Q \tag{9.12}$$

where the local capacity

$$G_{1,n^{\text{mem}}}^{\text{Str},q}(\boldsymbol{x}) = \begin{cases} \dfrac{F_{n^{\text{mem}}}^{q}(\boldsymbol{x})}{A_{\text{e},n^{\text{mem}}}(x_{i,j})\,p_{\text{y},n^{\text{mem}}}(x_{i,j})} + \dfrac{M_{\text{X},n^{\text{mem}}}^{q}(\boldsymbol{x})}{M_{\text{CX},n^{\text{mem}}}(x_{i,j})} + \dfrac{M_{\text{Y},n^{\text{mem}}}^{q}(\boldsymbol{x})}{M_{\text{CY},n^{\text{mem}}}(x_{i,j})} & \text{for tension members} \\[2ex] \dfrac{F_{n^{\text{mem}}}^{q}(\boldsymbol{x})}{A_{\text{g},n^{\text{mem}}}(x_{i,j})\,p_{\text{y},n^{\text{mem}}}(x_{i,j})} + \dfrac{M_{\text{X},n^{\text{mem}}}^{q}(\boldsymbol{x})}{M_{\text{CX},n^{\text{mem}}}(x_{i,j})} + \dfrac{M_{\text{Y},n^{\text{mem}}}^{q}(\boldsymbol{x})}{M_{\text{CY},n^{\text{mem}}}(x_{i,j})} & \text{for comprisson members} \end{cases} \tag{9.13}$$

where $F_{n^{\text{mem}}}^{q}(\boldsymbol{x})$ is the axial force. The applied moment about the local axes X and Y are $M_{\text{X},n^{\text{mem}}}^{q}(\boldsymbol{x})$ and $M_{\text{Y},n^{\text{mem}}}^{q}(\boldsymbol{x})$. The design strength is $p_{\text{y},n^{\text{mem}}}(x_{i,j})$. The moment capacities of the member about its X and Y axes are $M_{\mathrm{CX},n^{\mathrm{mem}}}(x_{i,j})$ and $M_{\mathrm{CY},n^{\mathrm{mem}}}(x_{i,j})$. It is assumed that $A_{\mathrm{e},n^{\mathrm{mem}}}(x_{i,j})$ and $A_{\mathrm{g},n^{\mathrm{mem}}}(x_{i,j})$ are equal.

According to clause 4.3.7 of BS 5950, the designer is not required to check the bracing members for lateral torsional buckling when they are in tension, therefore the overall capacity $G^{\mathrm{Str},q}_{2,n^{\mathrm{mem}}}(\boldsymbol{x})$ is determined by

$$G^{\mathrm{Str},q}_{2,n^{\mathrm{mem}}}(\boldsymbol{x})=\begin{cases}\dfrac{m^{q}_{n^{\mathrm{mem}}}(\boldsymbol{x})\,M^{q}_{\mathrm{X},n^{\mathrm{mem}}}(\boldsymbol{x})}{M_{\mathrm{b},n^{\mathrm{mem}}}(\boldsymbol{x})} & \text{for tension members (beams and columns)}\\[2ex] \dfrac{F^{q}_{n^{\mathrm{mem}}}(\boldsymbol{x})}{A_{\mathrm{g},n^{\mathrm{mem}}}(x_{i,j})\,p_{\mathrm{C},n^{\mathrm{mem}}}(x_{i,j})}+\dfrac{m^{q}_{n^{\mathrm{mem}}}(\boldsymbol{x})\,M^{q}_{\mathrm{X},n^{\mathrm{mem}}}(\boldsymbol{x})}{M_{\mathrm{b},n^{\mathrm{mem}}}(\boldsymbol{x})}+ & \\ \qquad\dfrac{m^{q}_{n^{\mathrm{mem}}}(\boldsymbol{x})\,M^{q}_{\mathrm{Y},n^{\mathrm{mem}}}(\boldsymbol{x})}{p_{\mathrm{y},n^{\mathrm{mem}}}(x_{i,j})\,Z_{\mathrm{Y},n^{\mathrm{mem}}}(x_{i,j})} & \text{for compression members.}\end{cases} \tag{9.14}$$

The shear capacities $G^{\mathrm{Str},q}_{3,n^{\mathrm{mem}}}(\boldsymbol{x})$ and $G^{\mathrm{Str},q}_{4,n^{\mathrm{mem}}}(\boldsymbol{x})$ are computed by

$$G^{\mathrm{Str},q}_{3,n^{\mathrm{mem}}}(\boldsymbol{x})=\frac{F^{q}_{\mathrm{X},n^{\mathrm{mem}}}(\boldsymbol{x})}{P_{\mathrm{X},n^{\mathrm{mem}}}(x_{i,j})}, \tag{9.15}$$

$$G^{\mathrm{Str},q}_{4,n^{\mathrm{mem}}}(\boldsymbol{x})=\frac{F^{q}_{\mathrm{Y},n^{\mathrm{mem}}}(\boldsymbol{x})}{P_{\mathrm{Y},n^{\mathrm{mem}}}(x_{i,j})} \tag{9.16}$$

where $P_{\mathrm{X},n^{\mathrm{mem}}}(x_{i,j})$ and $P_{\mathrm{Y},n^{\mathrm{mem}}}(x_{i,j})$ are the shear capacities of the member in the X and Y directions. The critical shear forces are $F^{q}_{\mathrm{X},n^{\mathrm{mem}}}(\boldsymbol{x})$.

Each member should also checked for shear buckling $G^{\mathrm{Str},q}_{5,n^{\mathrm{mem}}}(\boldsymbol{x})$ if

$$\frac{d(x_{i,j})}{t(x_{i,j})}\geq 63\,\varepsilon(x_{i,j}). \tag{9.17}$$

Hence,
$$G^{\mathrm{Str},\,q}_{4,\,n^{\mathrm{mem}}}(\boldsymbol{x}) = \frac{F^{q}_{\mathrm{Y},\,n^{\mathrm{mem}}}(\boldsymbol{x})}{V_{\mathrm{cr},\,n^{\mathrm{mem}}}(x_{i,\,j})}. \tag{9.18}$$

d) For a sway structure, the notional horizontal loading case is considered, this is termed the sway stability criterion.

<u>Step 8.</u> Checks of the horizontal (in X' and Y' directions) and vertical nodal displacements that are known as serviceability criteria

$$G^{\mathrm{Ser}}_{t,\,n^{\mathrm{mem}}}(\boldsymbol{x}) \leq 1,\; t = 1,\, 2 \text{ and } 3. \tag{9.19}$$

This is performed by:

a) Computing the horizontal nodal displacements due to the unfactored imposed loads and wind loading cases in order to satisfy the limits on the horizontal displacements,

$$G^{\mathrm{Ser}}_{1,\,n^{\mathrm{mem}}_{\mathrm{c}}} = \frac{\left|\Delta^{\mathrm{U}}_{\mathrm{X}',\,n^{\mathrm{mem}}_{\mathrm{c}}}(\boldsymbol{x}) - \Delta^{\mathrm{L}}_{\mathrm{X}',\,n^{\mathrm{mem}}_{\mathrm{c}}}(\boldsymbol{x})\right|}{\left(\dfrac{L_{n^{\mathrm{mem}}_{\mathrm{c}}}}{300}\right)}, \tag{9.20}$$

$$G^{\mathrm{Ser}}_{2,\,n^{\mathrm{mem}}_{\mathrm{c}}} = \frac{\left|\Delta^{\mathrm{U}}_{\mathrm{Y}',\,n^{\mathrm{mem}}_{\mathrm{c}}}(\boldsymbol{x}) - \Delta^{\mathrm{L}}_{\mathrm{Y}',\,n^{\mathrm{mem}}_{\mathrm{c}}}(\boldsymbol{x})\right|}{\left(\dfrac{L_{n^{\mathrm{mem}}_{\mathrm{c}}}}{300}\right)} \text{ and } n^{\mathrm{mem}}_{\mathrm{c}} = 1, \Lambda\, , N^{\mathrm{mem}}_{\mathrm{c}}. \tag{9.21}$$

b) Imposing the limits on the vertical nodal displacements (maximum value within a beam) due to the unfactored imposed loading case using

$$G^{\mathrm{Ser}}_{2,\,n^{\mathrm{mem}}_{\mathrm{b}}}(\boldsymbol{x}) = \frac{\left|\delta^{\max}_{n^{\mathrm{mem}}_{\mathrm{b}}}(\boldsymbol{x})\right|}{\left(\dfrac{L_{n^{\mathrm{mem}}_{\mathrm{b}}}}{360}\right)},\; n^{\mathrm{mem}}_{\mathrm{b}} = 1, 2, \Lambda\, , N^{\mathrm{mem}}_{\mathrm{b}}. \tag{9.22}$$

The flowchart given in Figure 9.3 illustrates the design procedure of 3D steel frame structures to BS 5950.

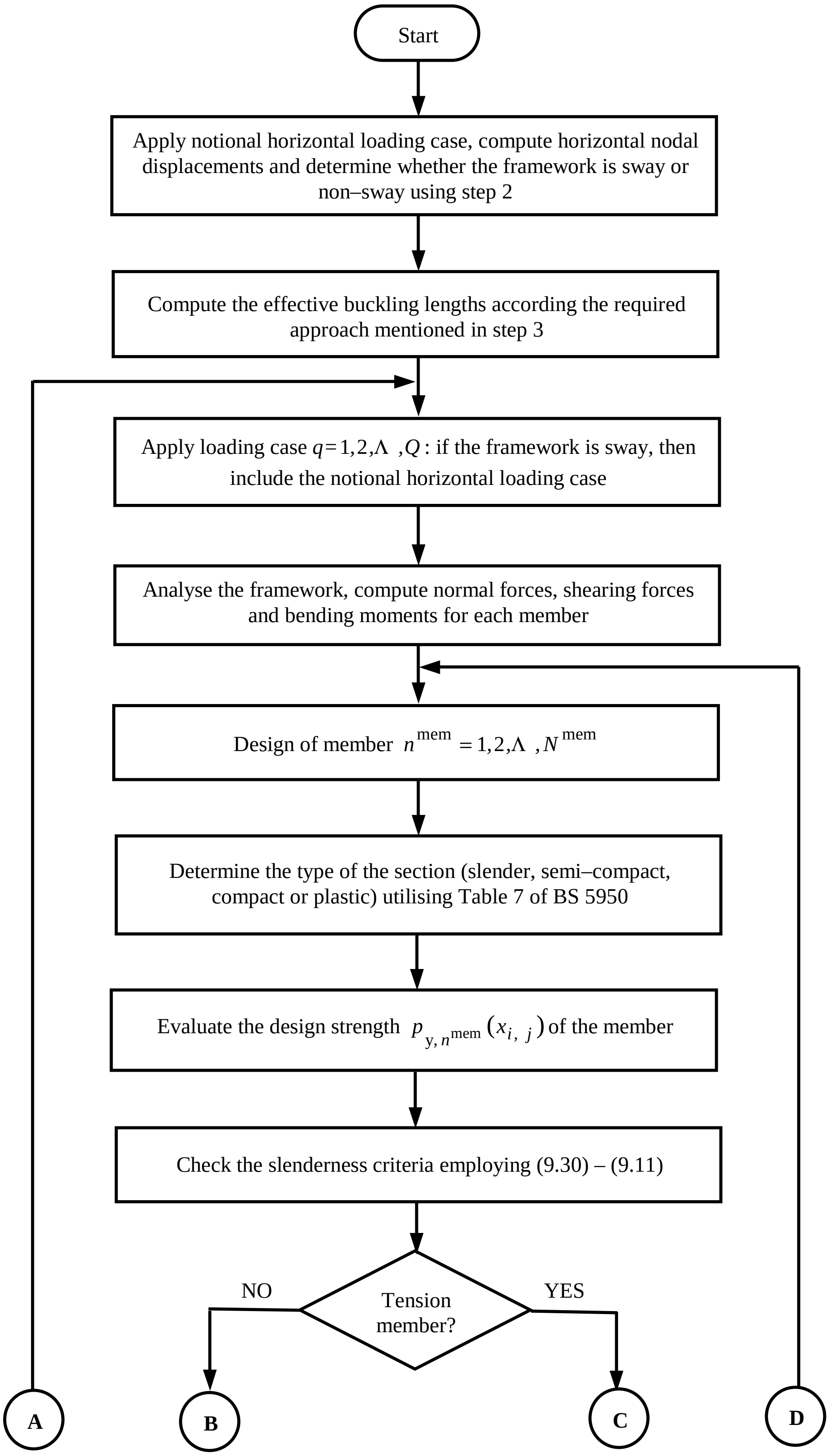

Figure 9.3a. Flowchart of design procedure of 3D steel frame structures

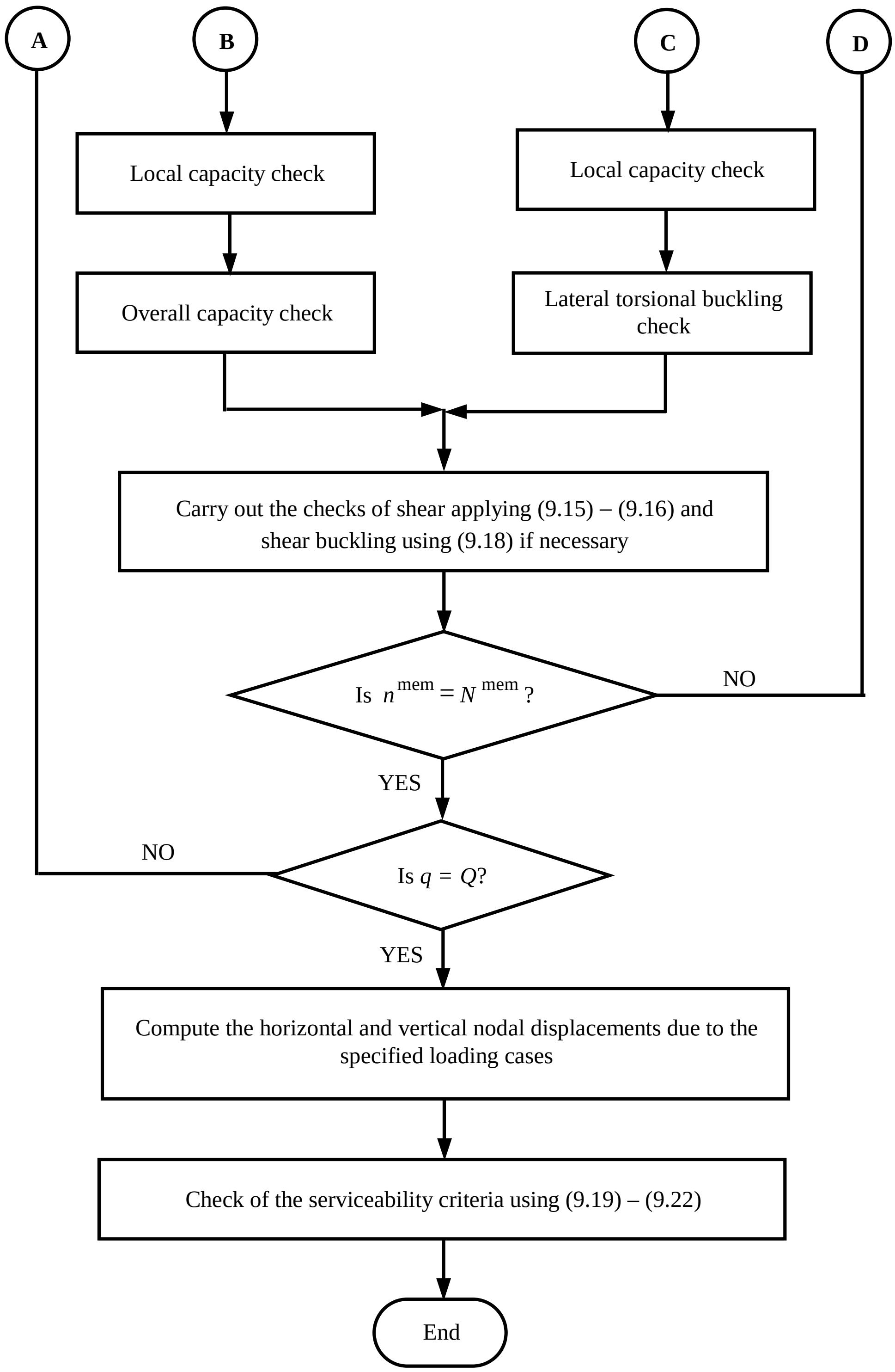

Figure 9.3b. (cont.) Flowchart of design procedure of 3D steel frame structures

9.3 Problem formulation and solution technique

The general formulation of the design optimization problem can be expressed by

$$\text{Minimize } F(\boldsymbol{x}) = \sum_{n^{\text{mem}}=1}^{N^{\text{mem}}} W_{n^{\text{mem}}} L_{n^{\text{mem}}}$$

$$\text{subject to: } G^{\text{Str},q}_{r,n^{\text{mem}}}(\boldsymbol{x}) \le 1,\ r = 1, 2, 3, 4,\ q = 1, 2, \Lambda\ , Q$$

$$G^{\text{Sle}}_{s,n^{\text{mem}}}(\boldsymbol{x}) \le 1,\ s = 1, 2$$

$$G^{\text{Ser}}_{t,n^{\text{mem}}}(\boldsymbol{x}) \le 1,\ t = 1, 2, 3$$

$$\frac{I_{\text{x}}^{n_{\text{s}},n_{\text{b}}}}{I_{\text{x}}^{n_{\text{s}}-1,n_{\text{b}}}} \le 1,\ n_{\text{s}} = 1, 2, \Lambda\ , N_{\text{s}},\ n_{\text{b}} = 1, 2, \Lambda\ , N_{\text{b}} + 1 \qquad (9.23)$$

$$\boldsymbol{x} = (\boldsymbol{x}_1^T, \boldsymbol{x}_2^T, \boldsymbol{x}_j^T, \Lambda\ , \boldsymbol{x}_J^T),\ j = 1, 2, \Lambda\ , J$$

$$x_{i,j} \in D_j \text{ and}$$

$$D_j = (d_{j,1}, d_{j,2}, \Lambda\ , d_{j,\lambda})$$

where $W_{n^{\text{mem}}}$ is the mass per unit length of the member under consideration and is taken from a catalogue. The strength, slenderness and serviceability criteria are $G^{\text{Str},q}_{r,n^{\text{mem}}}(\boldsymbol{x})$, $G^{\text{Sle}}_{s,n^{\text{mem}}}(\boldsymbol{x})$ and $G^{\text{Ser}}_{t,n^{\text{mem}}}(\boldsymbol{x})$ respectively. The vector of design variables $\boldsymbol{x}$ is divided into J sub–vectors $\boldsymbol{x}_J$. The components of these sub–vectors take values from a corresponding catalogue D_j. In the present work, the cross–sectional properties of the structural members, which form the design variables, are chosen from three separate catalogues (universal beams and columns covered by BS 4, and circular hollow sections from BS 4848). Figure 9.4 demonstrates the applied solution technique.

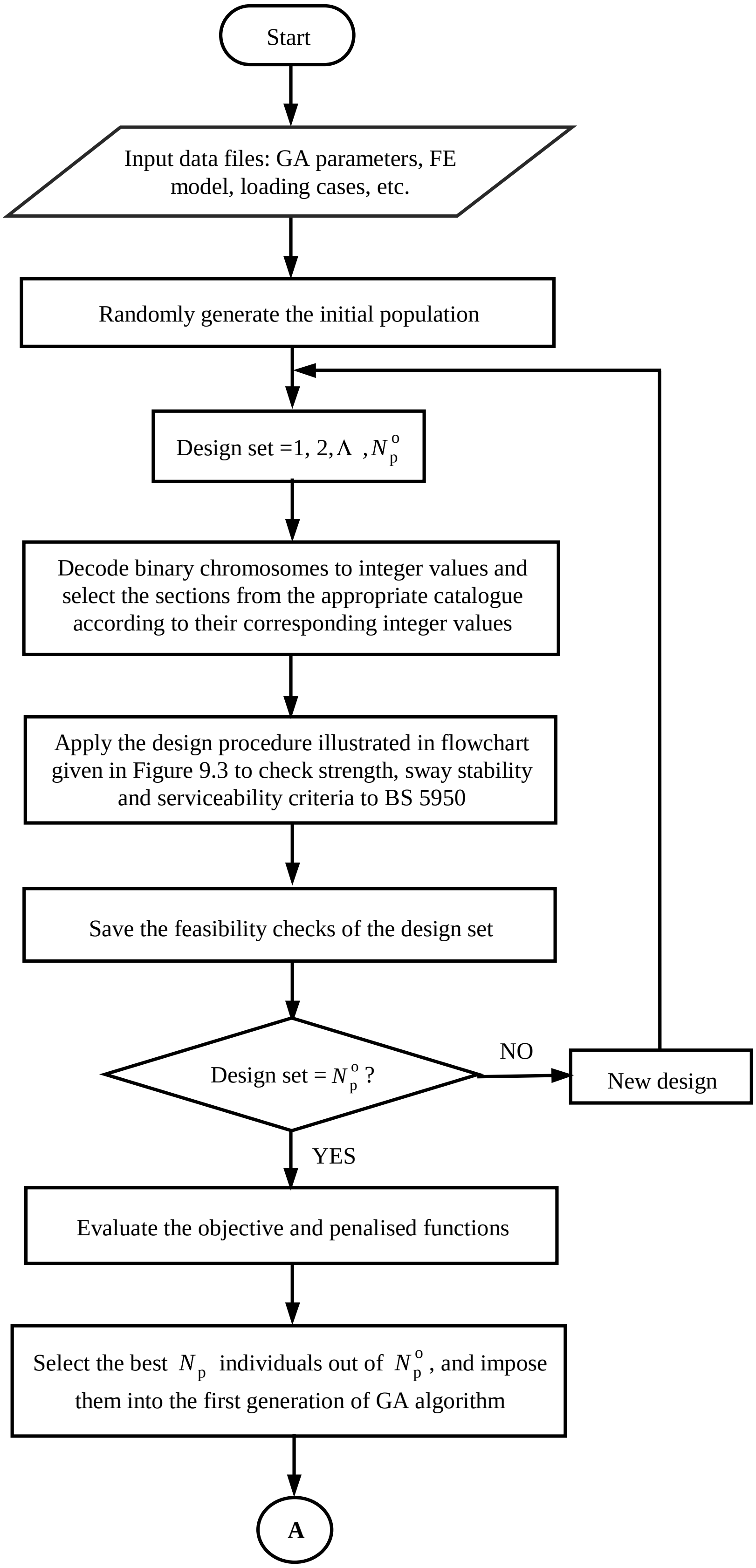

Figure 9.4a. Flowchart for the solution technique

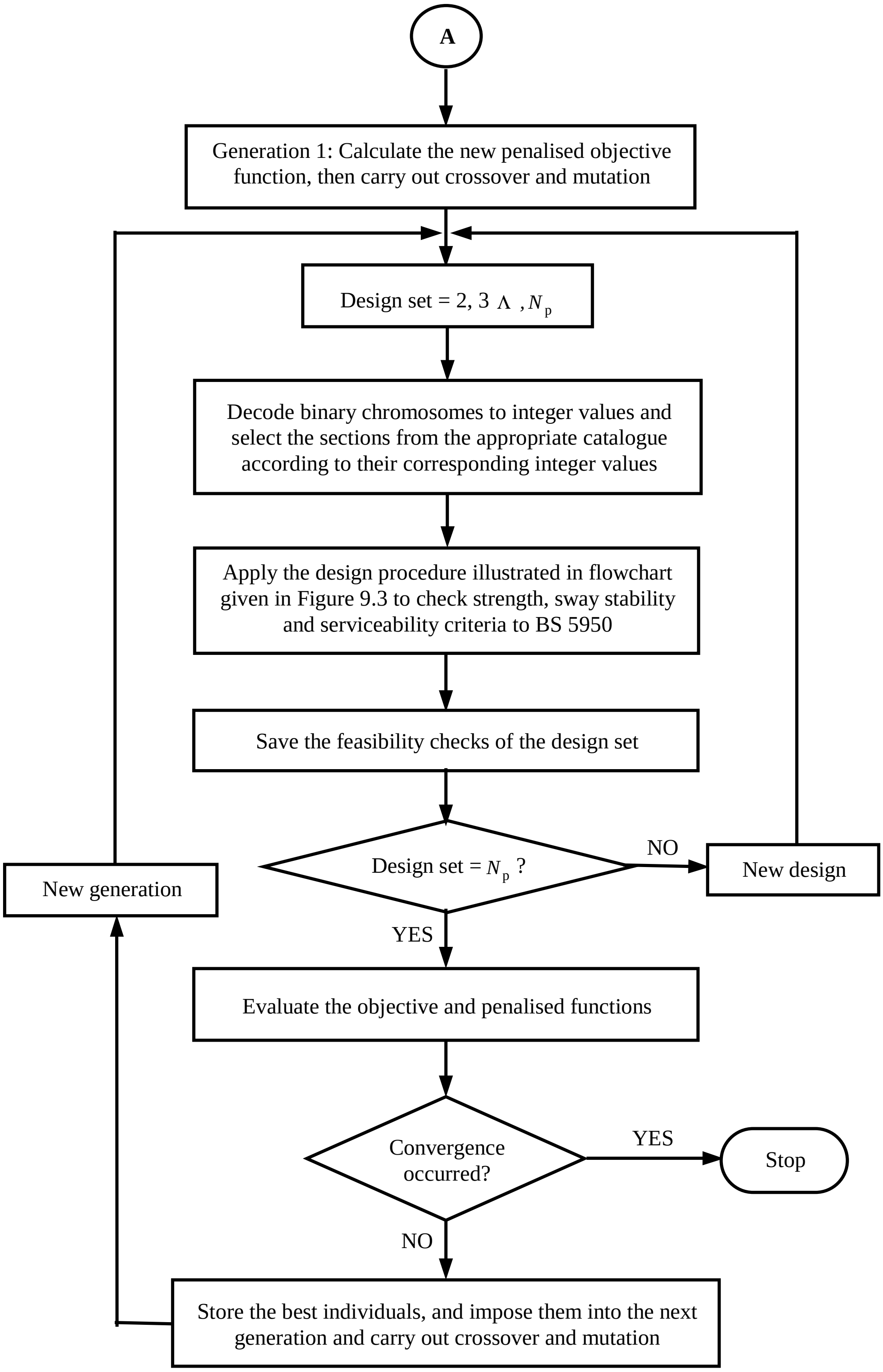

Figure 9.4b. (cont.) Flowchart for the solution technique

9.4 Benchmark examples

Having introduced the design procedure according to BS 5950 linked to the GA procedure and the formulation of design optimization problem, the process of optimization in now carried out.

Two steel frame structures are demonstrated here to illustrate the effectiveness and benefits of the developed GA technique as well as investigating the effect of the employed approach for the determination of the effective buckling length on the optimum design attained.

The catalogue of available cross sections in BS 4 include 64 universal beams (UB) and 32 universal columns (UC). These sections are given in Section 7.2.1. The catalogue of circular hollow sections (CHS) is taken from BS 4848 and this includes 64 sections, listed in Table 9.1, varying from 76.1 $\times$ 5.0 CHS to 457.0 $\times$ 40.0 CHS.

In the present work, the initial population size $N_{\mathrm{p}}^{\mathrm{o}}$ is assumed to be 1000 and fixed population size N_{p} of 70 during successive generations, elite percentage E_{r} was 30 %, probability of crossover P_{c} was 0.7, probability of mutation P_{m} was 0.01 and one–point crossover is applied. In addition, the technique described in Section 6.2 is utilised where the simple "exact" penalty function employed is

$$\text{Minimize } \overline{F}(\boldsymbol{x}) = \begin{cases} \mathrm{C} - F(\boldsymbol{x}), & \text{all constraints satisfied} \\ 0\,, & \text{any of constraints violated.} \end{cases} \tag{9.24}$$

The convergence criteria and termination conditions detailed in Section 5.6.3.7 are used where C^{av} = 0.001, C^{cu} = 0.001 and $gen^{\max} = 200$.

Table 9.1. The used circular hollow sections

	Cross section		Cross section		Cross section
1	76.1 × 5.0 CHS	23	219.1 × 10.0 CHS	45	323.9 × 25.0 CHS
2	88.9 × 3.2 CHS	24	219.1 × 12.5 CHS	46	355.6 × 8.0 CHS
3	88.9 × 4.0 CHS	25	219.1 × 16.0 CHS	47	355.6 × 10.0 CHS
4	88.9 × 5.0 CHS	26	219.1 × 20.0 CHS	48	355.6 × 12.5 CHS
5	114.3 × 3.6 CHS	27	244.5 × 6.3 CHS	49	355.6 × 16.0 CHS
6	114.3 × 5.0 CHS	28	244.5 × 8.0 CHS	50	355.6 × 20.0 CHS
7	114.3 × 6.3 CHS	29	244.5 × 10.0 CHS	51	355.6 × 25.0 CHS
8	139.7 × 5.0 CHS	30	244.5 × 12.5 CHS	52	406.4 × 10.0 CHS
9	139.7 × 6.3 CHS	31	244.5 × 16.0 CHS	53	406.4 × 12.5 CHS
10	139.7 × 8.0 CHS	32	244.5 × 20.0 CHS	54	406.4 × 16.0 CHS
11	139.7 × 10.0 CHS	33	273.0 × 6.3 CHS	55	406.4 × 20.0 CHS
12	168.3 × 5.0 CHS	34	273.0 × 8.0 CHS	56	406.4 × 25.0 CHS
13	168.3 × 6.3 CHS	35	273.0 × 10.0 CHS	57	406.4 × 32.0 CHS
14	168.3 × 8.0 CHS	36	273.0 × 12.5 CHS	58	457.0 × 10.0 CHS
15	168.3 × 10.0 CHS	37	273.0 × 16.0 CHS	59	457.0 × 12.5 CHS
16	193.7 × 6.3 CHS	38	273.0 × 20.0 CHS	60	457.0 × 16.0 CHS
17	193.7 × 8.0 CHS	39	273.0 × 25.0 CHS	61	457.0 × 20.0 CHS
18	193.7 × 10.0 CHS	40	323.9 × 8.0 CHS	62	457.0 × 25.0 CHS
19	193.7 × 12.5 CHS	41	323.9 × 10.0 CHS	63	457.0 × 32.0 CHS
20	193.7 × 16.0 CHS	42	323.9 × 12.5 CHS	64	457.0 × 40.0 CHS
21	219.1 × 6.3 CHS	43	323.9 × 16.0 CHS		
22	219.1 × 8.0 CHS	44	323.9 × 20.0 CHS		

9.4.1 Example 1: Two–bay by two–bay by two–storey structure

The first 3D steel frame structure, analysed in this chapter, is the two–bay by two–bay by two–storey structure shown in Figure 9.5. It can be observed from Figure 9.5a that the structure consists of three successive frameworks, transverse beams and the bracing system. The spacing between the successive frameworks is 10.0 m while the distance between the successive transverse beams is 5 m.

Because BS 5950 does not cater for the design of members subjected to torsional moments, it is assumed that one end of each transverse beam is free to rotate about its local axes X, Y and Z while the second end is free to rotate about X and Y axes. Similarly, the structural system of the bracing members is considered. The structural system is shown in Figures 9.5b–9.5d.

The structure was designed for use as an office block including projection rooms. Nine loading cases were taken into account and these represent the most unfavourable combinations of the factored dead load (*DL*), imposed load (*LL*) and wind load (*WL*) as required by BS 5950 and BS 6399. Because the structure is doubly–symmetric, two orthogonal wind cases have been considered where the wind loads are factored by 1.2. The values of the unfactored *DL* and *LL* are tabulated in Table 9.2. These values are calculated according to the recommendations given by Owens et al (1992), MacGinley (1997) and Nethercot (1995).

Table 9.2. The values of dead load and imposed load

	Value of the load on roof	**Value of the load on first floor**
DL	7.0 kN/m^2	9.0 kN/m^2
LL	2.0 kN/m^2	5.0 kN/m^2

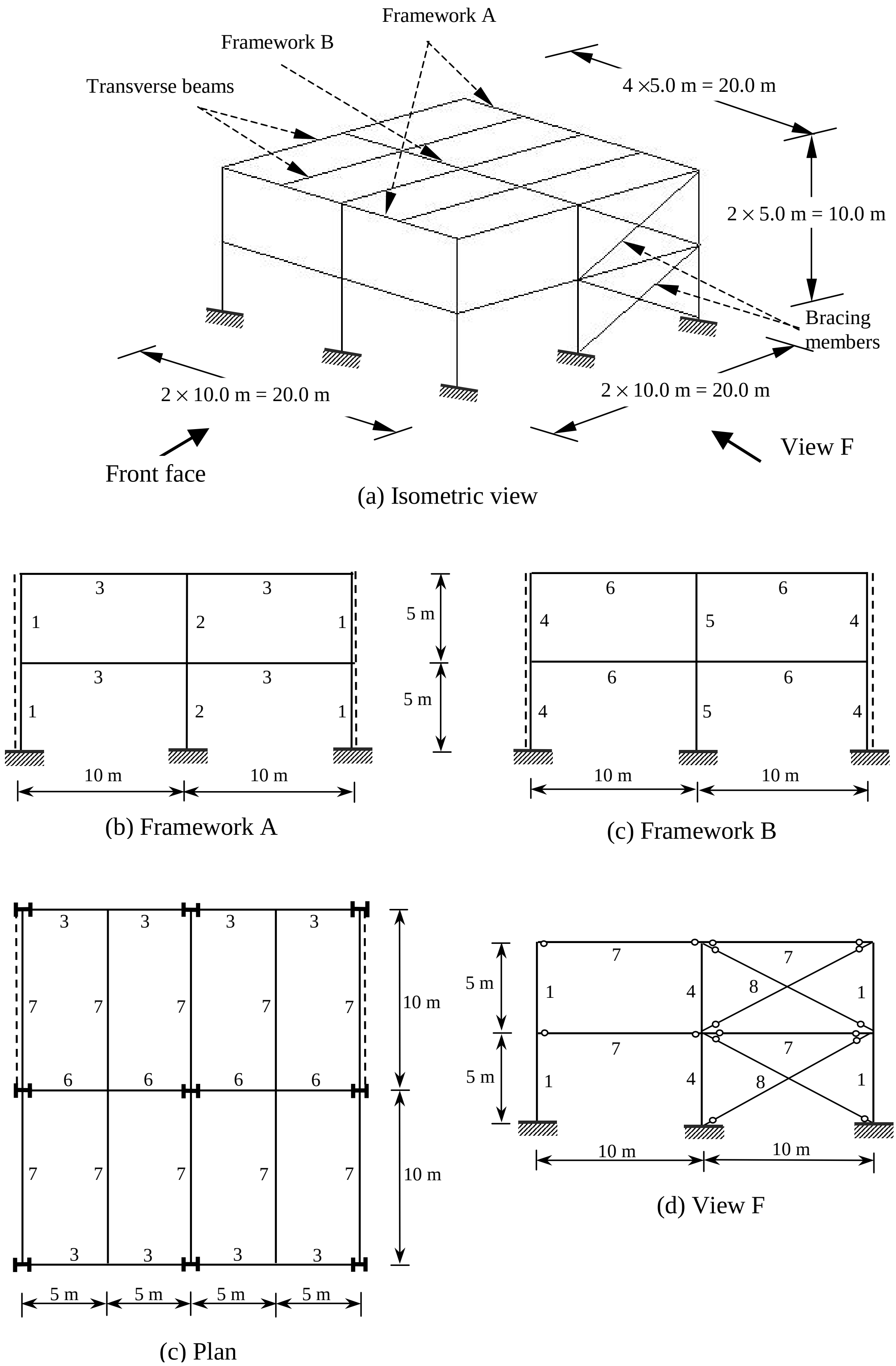

Figure 9.5. Two–bay by two–bay by two–storey structure

The reinforced concrete slabs are assumed to transmit the loads in one direction because the ratio of the spacing between the successive frameworks and the distances between the successive transverse beams equal 2 (see MacGinley, 1997).

According to BS 6399: Part 2, the standard method was utilised to determine the values of the wind pressures on the vertical walls and the flat roof assuming

1. the openings are dominant,
2. the building type factor equal 4.0,
3. the reference height of the structure (H_r) equal to the maximum height of the structure above the ground level (10.0 m),
4. the basic wind speed V_b is 23 m/s,
5. the terrain and building factor S_b is 1.58,
6. the altitude factor S_a, the directional factor S_d, the seasonal factor S_s and the probability factor S_p equal 1.0,
7. the size effect factor C_a is taken as 0.90,
8. the external pressure coefficient C_{pe} for each surface of the building is determined according table 5 and 8 of BS 6399 and
9. the internal pressure coefficient C_{pi} for each surface of the structure is

$$C_{pi} = 0.75\, C_{pe} \tag{9.25}$$

where C_{pe} is the external pressure coefficient of the surface under consideration.

At this stage having introduced the basic assumptions for evaluating the design loads, the values of these loads can accordingly be computed depending on the nine loading cases summarised bellow:

1. the floors are subjected to the vertical uniform loads $P^{v} = 1.4DL + 1.6LL$,

2. the floors are subjected to the vertical uniform loads $P^{v} = 1.4DL + 1.6LL$, and left hand side (LHS) nodes of each framework are subjected to the horizontal concentrated loads due to the notional horizontal loading condition,
3. the floors of the first bay (counting from the left) are subjected to the vertical uniform loads $P^{v} = 1.4DL$ while the rest of the floors are subjected to $P^{v} = 1.4DL + 1.6LL$,
4. the floors are subjected to a staggered arrangement of vertical uniform loads $P^{v} = 1.4DL + 1.6LL$ and $P^{v} = 1.4DL$,
5. the floors are subjected to the vertical uniform loads $P^{v} = 1.2DL + 1.2LL$ and the structure is subjected to the first factored wind loading case when the LHS face of the structure is the windward face,
6. the floors are subjected to the vertical uniform loads $P^{v} = 1.2DL + 1.2LL$ and the structure is subjected to the second factored wind loading case when the front face of the structure is the windward face,
7. the floors are subjected to the vertical uniform load $P^{v} = 1.0LL$,
8. the floors are subjected to the vertical uniform loads $P^{v} = 1.0LL$ and the structure is subjected to the first unfactored wind loading case when the LHS face of the structure is the windward face and
9. the floors are subjected to the vertical uniform loads $P^{v} = 1.0LL$ and the structure is subjected to the second unfactored wind loading case when the front face of the structure is the windward face.

A more accurately evaluated effective buckling length of columns was determined using the finite element method using the loading pattern displayed in Figure 9.6. The finite element model of the structure was assembled in ANSYS using 5 elements for each beam and column while one element for each member of the bracing system was used.

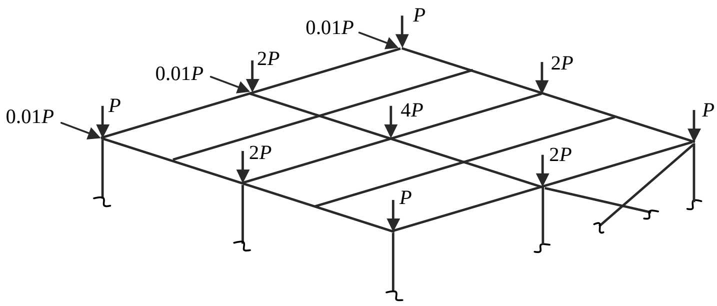

(a) Loading pattern of the roof level

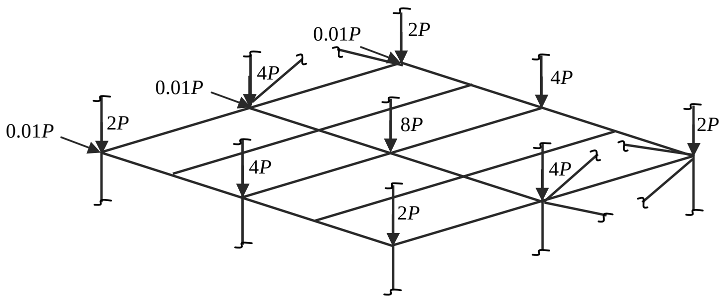

(b) Loading pattern of the first floor level

Figure 9.6. Loading pattern used for the stability analysis

The design optimization processes were carried out considering 8 design variables. The linking of the design variables is displayed in Figures 9.3.b–9.3d. Referring to BS 4 and BS 4848, the catalogue of the available cross sections includes 64 universal beams (UB), 32 universal columns (UC) and 64 circular hollow sections (CHS). This results in a total string length of 44.

The problem was analysed utilising the solution parameters as described in Section 9.4. Five runs of the design optimization processes were carried out using 5 different seed numbers to generate the initial population. Solutions are presented in Table 9.3. The design variables corresponding to the best designs are given in Table 9.4.

Table 9.3. Two–bay by two–bay by two–storey structure: comparison of the best design obtained in five runs

Run	Total weight (kg)		
	First approach (code)	**Second approach (FE)**	**Third approach (conservative)**
1	62023.89	69047.74	70856.30
2	62730.46	70563.89	72220.46
3	63079.28	69527.74	70547.74
4	63150.46	69867.74	70390.46
5	62730.46	70347.74	69383.89
Average weight	62742.91	69870.97	70679.77
Minimum weight	62023.89	69047.74	69383.89

Table 9.4. Two–bay by two–bay by two–storey structure: comparison of the design variables for the obtained optimum designs

Design variable	Cross sections		
	First approach (code)	**Second approach (FE)**	**Third approach (conservative)**
1	$203 \times 203 \times 52$ UC	$356 \times 368 \times 129$ UC	$356 \times 368 \times 129$ UC
2	$305 \times 305 \times 97$ UC	$356 \times 368 \times 129$ UC	$356 \times 368 \times 202$ UC
3	$356 \times 368 \times 129$ UC	$356 \times 368 \times 177$ UC	$356 \times 368 \times 177$ UC
4	$356 \times 368 \times 153$ UC	$356 \times 406 \times 393$ UC	$356 \times 406 \times 235$ UC
5	$686 \times 254 \times 125$ UB	$686 \times 254 \times 125$ UB	$686 \times 254 \times 125$ UB
6	$838 \times 292 \times 176$ UB	$914 \times 305 \times 201$ UB	$914 \times 305 \times 201$ UB
7	$762 \times 267 \times 173$ UB	$686 \times 254 \times 170$ UB	$686 \times 254 \times 170$ UB
8	168.3×6.3 CHS	168.3×5.0 CHS	168.3×6.3 CHS
Weight (kg)	62023.89	69047.74	69383.89

During the design optimization process, the convergence characteristics of the solutions were examined. Figure 9.7 shows the convergence history of the best designs. It can be observed that the best solutions were obtained within 50 generations while the rest of the computations were carried out to satisfy the convergence criteria.

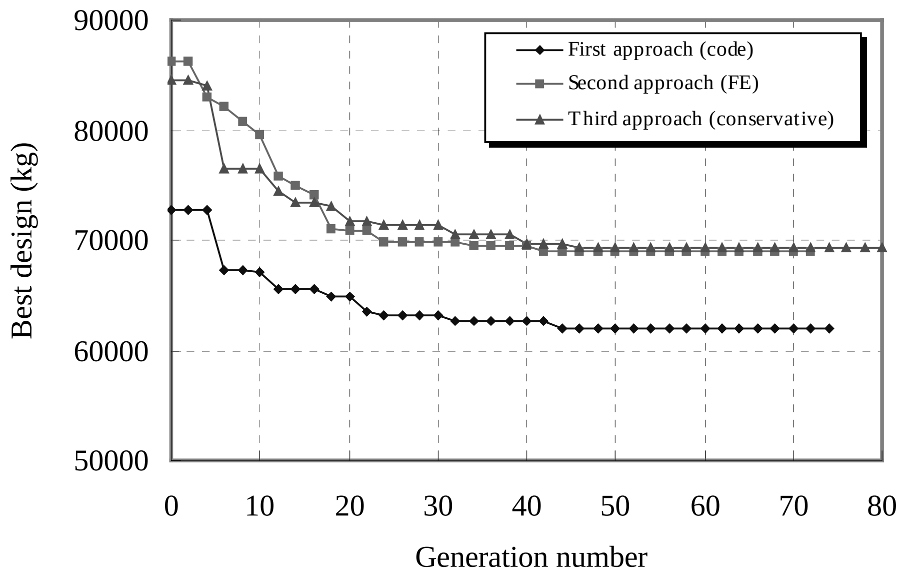

Figure 9.7. Two–bay by two–bay by two–storey structure: best design versus generation number

9.4.2 Example 2: Three–bay by four–bay by four–storey structure

The next 3D structure is the three–bay by four–bay by four–storey structure shown in Figure 9.8. The structure consists of four successive frameworks, transverse beams and a bracing system as shown in Figure 9.8a. The spacing between the successive frameworks is 8.0 m. The distance between the successive transverse beams is 4.0 m. The structural system is shown in Figures 9.8b–9.8f. The structure is designed for use as an office block including projection rooms. Ten loading cases representing the most unfavourable combinations of the factored *DL*, *LL* and *WL* are taken into account.

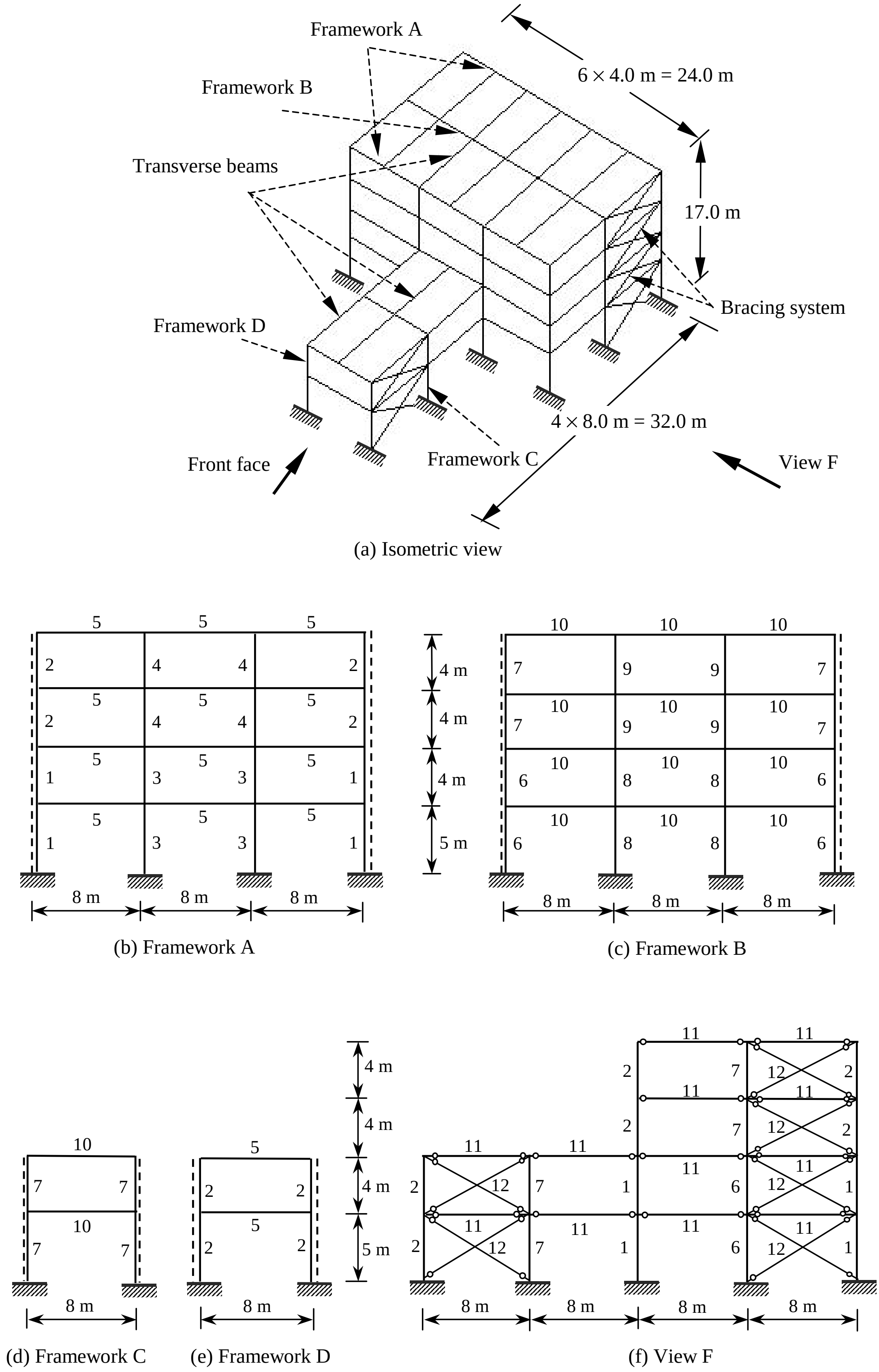

Figure 9.8. Three–bay by four–bay by four–storey structure

Because the structure is singly–symmetric, three orthogonal wind cases have been considered where the wind loads are factored by 1.2. The values of the unfactored *DL* and *LL* are tabulated in Table 9.2.

Table 9.5. The values of deal load and imposed load

	Value of the load on roof	**Value of the load on other floors**
DL	6.5 kN/m^2	8.0 kN/m^2
LL	2.0 kN/m^2	5.0 kN/m^2

According to BS 6399: Part 2, the standard method was utilised to determine the values of the wind pressures on the vertical walls and the flat roof considering:

1. the openings are dominant,
2. the building type factor equals 4.0,
3. the reference height of the structure (H_r) equals to the maximum height of the structure above the ground level (17.0 m),
4. the basic wind speed V_b is 23 m/s,
5. the terrain and building factor S_b is 1.71,
6. the altitude factor S_a, the directional factor S_d, the seasonal factor S_s and the probability factor S_p equal 1.0,
7. the size effect factor C_a is taken as 0.87,
8. the external pressure coefficient C_{pe} for each surface of the building is determined (see Section 2.3.3) according Tables 5 and 8 of BS 6399 and
9. the internal pressure coefficient C_{pi} is calculated by (9.25).

The design loads were computed according to the following loading cases:

1. the floors are subjected to the vertical uniform loads $P^{v} = 1.4DL + 1.6LL$,
2. the floors are subjected to the vertical uniform loads $P^{v} = 1.4DL + 1.6LL$, and left hand side (LHS) nodes of each framework are subjected to the horizontal concentrated loads due to the notional horizontal loading condition (see Chapter 2),
3. the floors of the first bay (counting from the left) are subjected to the vertical uniform loads $P^{v} = 1.4DL$ while the rest of the floors are subjected to $P^{v} = 1.4DL + 1.6LL$,
4. the floors are subjected to a staggered arrangement of vertical uniform loads $P^{v} = 1.4DL + 1.6LL$ and $P^{v} = 1.4DL$,
5. the floors are subjected to the vertical uniform loads $P^{v} = 1.2DL + 1.2LL$ and the structure is subjected to the first factored wind loading case when the LHS face of the structure is the windward face,
6. the floors are subjected to the vertical uniform loads $P^{v} = 1.2DL + 1.2LL$ and the structure is subjected to the second factored wind loading case when the front face of the structure is the windward face,
7. the floors are subjected to the vertical uniform loads $P^{v} = 1.2DL + 1.2LL$ and the structure is subjected to the third factored wind loading case when the rear face of the structure is the windward face,
8. the floors are subjected to the vertical uniform load $P^{v} = 1.0LL$,
9. the floors are subjected to the vertical uniform loads $P^{v} = 1.0LL$ and the structure is subjected to the first unfactored wind loading case when the LHS face of the structure is the windward face and

10. the floors are subjected to the vertical uniform loads $P^{\mathrm{v}} = 1.0LL$ and the structure is subjected to the second unfactored wind loading case when the front face of the structure is the windward face.

The finite element method was employed (see Toropov *et al.*, 1999) in order to evaluate the effective buckling length of columns. This was performed by utilising the loading pattern displayed in Figure 9.9. In the finite element model, the structure was assembled in ANSYS using 5 elements for each beam and column while one element for each member of the bracing system.

The optimization process was carried out considering 12 design variables. The linking of the design variables is displayed in Figures 9.8.b–9.8f.

Referring to BS 4 and BS 4848, the catalogue of the available cross sections include 64 universal beams (UB), 32 universal columns (UC) and 64 circular hollow sections (CHS). This results in a total string length of 64.

The problem was analysed utilising the solution parameters described in Section 9.4. Five runs of the optimization process were carried out using 5 different seed numbers to generate the initial population. The optimization process was terminated when any of the convergence criteria is satisfied. Solutions are presented in Table 9.6. The design variables corresponding to the best designs are given in Table 9.7.

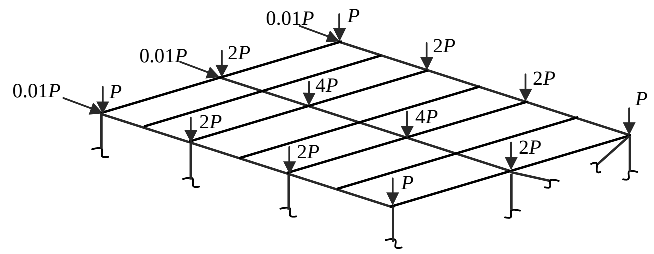

(a) Loading pattern of the roof level

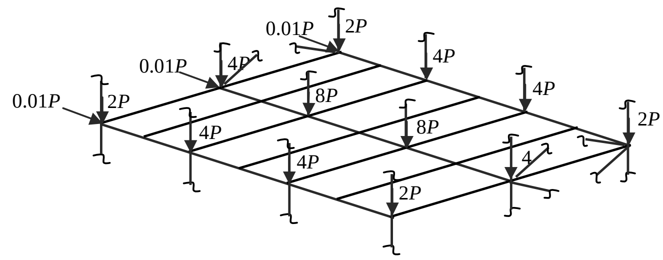

(b) Loading pattern of the third floor level

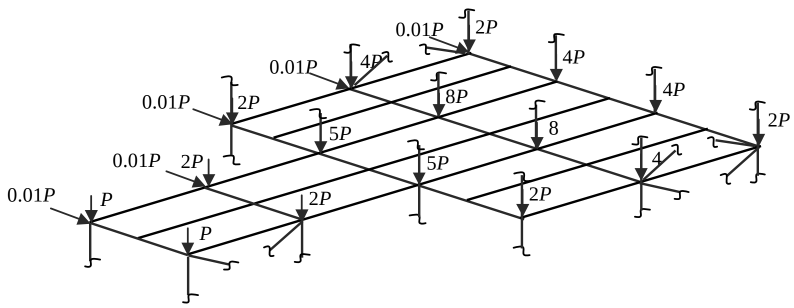

(c) Loading pattern of the second floor level

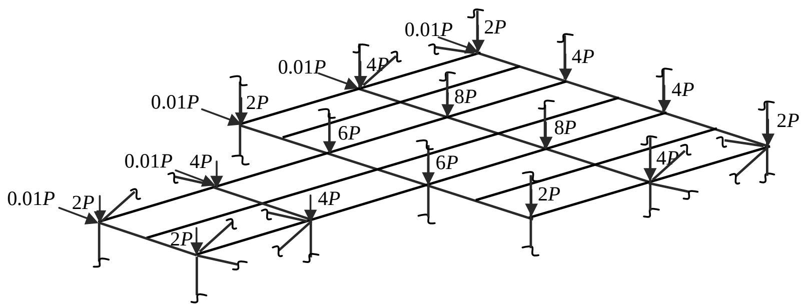

(d) Loading pattern of the first floor level

Figure 9.9. Loading pattern used for the stability analysis

Table 9.6. Three–bay by four–bay by four–storey structure: comparison of the best design obtained in five runs

Run	Total weight (kg)		
	First approach (code)	Second approach (FE)	Third approach (conservative)
1	168914.20	185520.60	188914.46
2	167214.50	185696.60	188522.56
3	169078.60	184881.00	187604.90
4	168492.20	185819.00	185566.40
5	169436.20	185852.60	188502.60
Average weight	168627.14	185553.96	187604.90
Minimum weight	167214.50	184881.00	185566.40

Table 9.7. Three–bay by four–bay by four–storey structure: comparison of the design variables for the obtained optimum designs.

Design variable	Cross sections		
	First approach (code)	Second approach (FE)	Third approach (conservative)
1	$305 \times 305 \times 137$ UC	$356 \times 368 \times 177$ UC	$356 \times 368 \times 177$ UC
2	$305 \times 305 \times 137$ UC	$356 \times 368 \times 177$ UC	$356 \times 368 \times 153$ UC
3	$356 \times 406 \times 235$ UC	$356 \times 406 \times 287$ UC	$356 \times 406 \times 287$ UC
4	$356 \times 406 \times 235$ UC	$356 \times 406 \times 287$ UC	$356 \times 406 \times 287$ UC
5	$686 \times 254 \times 125$ UB	$914 \times 305 \times 201$ UB	$914 \times 305 \times 201$ UB
6	$356 \times 368 \times 153$ UC	$356 \times 368 \times 153$ UC	$305 \times 305 \times 198$ UC
7	$356 \times 368 \times 153$ UC	$305 \times 305 \times 137$ UC	$356 \times 368 \times 153$ UC
8	$356 \times 406 \times 235$ UC	$356 \times 406 \times 340$ UC	$356 \times 406 \times 393$ UC
9	$356 \times 406 \times 235$ UC	$356 \times 406 \times 340$ UC	$356 \times 406 \times 393$ UC
10	$914 \times 305 \times 201$ UB	$686 \times 254 \times 140$ UB	$762 \times 267 \times 147$ UB
11	$686 \times 254 \times 125$ UB	$686 \times 254 \times 125$ UB	$686 \times 254 \times 125$ UB
12	139.7×10.0 CHS	139.7×8.0 CHS	139.7×5.0 CHS
Weight (kg)	167214.5	184881.00	185566.4

From Table 9.6, it can deduced that the optimizer was able to obtain several solutions and the differences between them are small.

During the optimization process, the convergence characteristics of the solutions were examined. Figure 9.10 shows the convergence history of the best designs.

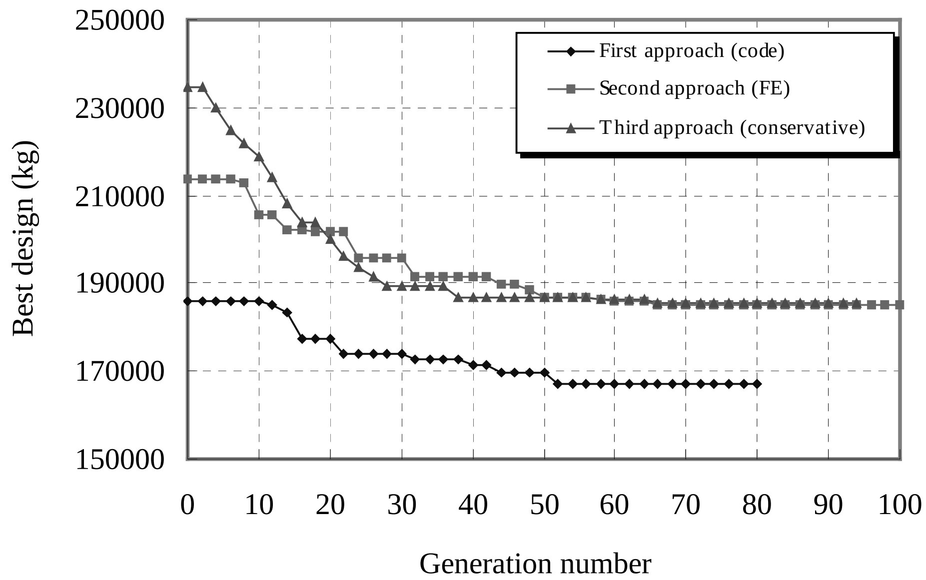

Figure 9.10. Three–bay by four–bay by four–storey structure: best design versus generation number.

From this figure, it can be observed that the optimum solutions were achieved within 50 generations while the rest of the computational effort was needed to satisfy the termination conditions described in section 9.4.

9.5 Validation of the optimum design

This section shows that the developed FORTRAN code for design of 3D steel frame structures is successfully implemented. As discussed in Section 8.5, to validate the applied FORTRAN code, the problem should be first run when $m^{q}_{n^{\mathrm{mem}}}$ is 1 (technique 2). Then, CSC software is used to check the calculated constraints.

The two–bay by two–bay by two–storey structure (studied in Section 9.4.1) was analysed. The loading cases mentioned in Section 9.4.1 are utilised. The optimization process was carried out using the design procedure discussed in Section 9.2 while the solution parameters and the convergence criteria were applied as considered in Section 9.4. Five runs were carried out when applying the first approach for determining the effective buckling lengths. The design variables corresponding to the best solution are tabulated in Table 9.8. It is worth comparing the design variables obtained with those achieved in section 9.4.1 (technique 1) when a more accurate equation for determining $m^{q}_{n_{\mathrm{mem}}}(\boldsymbol{x})$ was applied. This comparison is also presented in Table 9.8.

It can be observed that when applying technique 2, the optimizer succeeded in obtaining a solution (62570.47 kg) quite near to that achieved when using technique 1 (62023.89 kg).

Table 9.8. Two–bay by two–bay by two–storey structure: comparison of the design variables for the optimum designs.

Design variable	**Cross sections**	
	Technique 1	**Technique 2**
1	$203 \times 203 \times 52$ UC	$254 \times 254 \times 73$ UC
2	$305 \times 305 \times 97$ UC	$254 \times 254 \times 73$ UC
3	$356 \times 368 \times 129$ UC	$305 \times 305 \times 97$ UC
4	$356 \times 368 \times 153$ UC	$356 \times 368 \times 153$ UC
5	$686 \times 254 \times 125$ UB	$686 \times 254 \times 125$ UB
6	$838 \times 292 \times 176$ UB	$838 \times 292 \times 194$ UB
7	$762 \times 267 \times 173$ UB	$686 \times 292 \times 170$ UB
8	168.3×6.3 CHS	219.1×6.3 CHS
Weight (kg)	62023.89	62570.46

The convergence characteristics were also examined. This was achieved by plotting the changes of the best design with the number of generations performed for each run as shown in Figure 9.11.

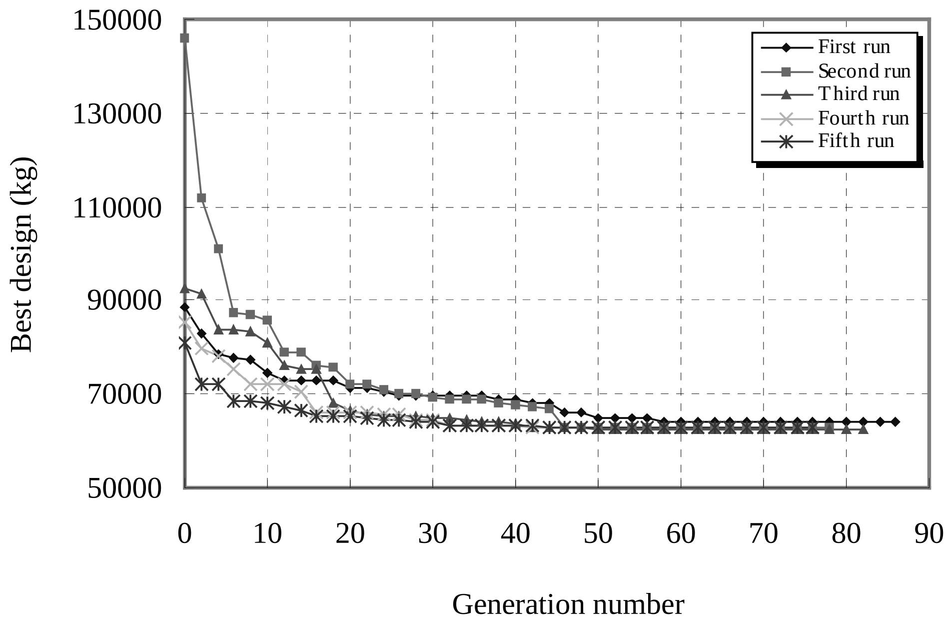

Figure 9.11. Two–bay by two–bay by two–storey structure: best design versus generation number

At this stage, the structural weight has been optimized and the section of each member has been determined. The next step is to validate the code checks using CSC software. This is achieved by using the following proceduce:

1) In S–FRAME, the structural geometry, member sections and loading cases are defined. Then, the bending moments, shear forces, and nodal displacements are calculated according to the analysis type presupposed (linear analysis).
2) Starting the S–STEEL program. The design checks are then carried out.
3) The design results are then displayed on a separate window as shown in Figure 9.12.

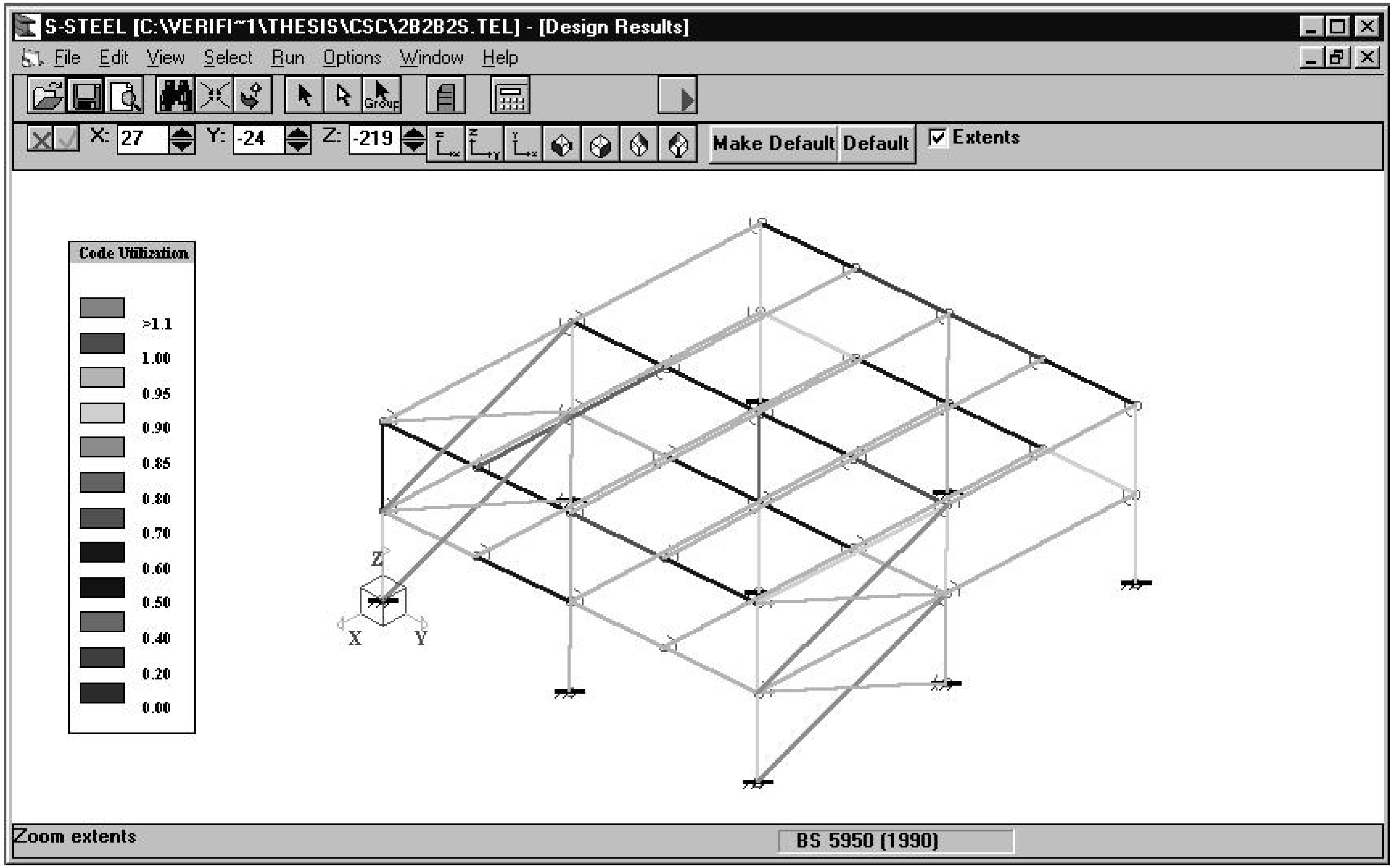

Figure 9.12. The design results of two–bay by two–bay by two–storey structure (captured from S–STEEL)

In this figure, the design checks of each member are indicated in colour in which the code utilisation menu gives the range for of each colour. It can be observed that most of the members reach their maximum capacities. This indicates that the developed algorithm is successfully incorporated in design optimization. It is worth noting that the design results vary between 0.7 and 1.0.

9.6 Concluding remarks

Design optimization technique based on GA was presented for 3D steel frame structures where the structures were subjected to multiple loading conditions. The design method obtained a 3D steel frame structure with the least weight by selecting appropriate sections for beams, columns and bracing members from the British standard for universal beam sections, universal column sections and circular hollow sections. The following concluding remarks can be made.

1) It has been proven that the developed GA approach can be successfully incorporated in design optimization in which the structural members have to be selected from the available standard sections while the design satisfies the design criteria. This indicates that the developed approach can be utilised by a practising designers.
2) In the present chapter, the skills and experience of the designer have been reflected in the optimization problem by imposing constraints on the second moment of area of two adjacent columns in two adjacent storey levels. This can be implemented using other constraints such as sectional dimensions, sectional area, etc. This indicates that the optimizer is able to treat different practical constraints depending on the nature of the problem.
3) It has been shown that the developed GA provides the designer with more than one solution to choose from, and the difference between them was small. This could be

an advantage when a designer needs to choose an appropriate solution depending on the availability of the sections.

4) From Tables 9.4 and 9.7, it can be observed that the same sections have been obtained for different members of a structure even though these members are linked to different design variables. This indicates that it can be beneficial to include the grouping of structural members as an additional criterion in the formulation of the design optimization problem.

5) In the present study, computation of the effective buckling length has been automated and included in the developed algorithm. This was achieved by employing three different approaches.

Application of a modified GA to design optimization of structural steelwork allows the best set from an appropriate catalogue of steel cross sections to be chosen. The optimizer has been linked to a commercial finite element code and the British codes of practice in order to obtain optimum designs accepted by practising structural engineers.